e-ISSN: 2689-4934

PENERBIT PRESS
UNIVERSITI TEKNOLOGI MARA

Available online at
http://uppp.uitm.edu.my/online-issues.html

ESTEEM Academic Journal Vol 22, September 2026, 98-111

ESTEEM
Academic Journal
(EAJ)

Structural and compositional characteristics of electrodeposited indium-modified tin (Sn/In) electrodes at different indium concentrations

Nur Basiroh Mohd Rahim[1], Norain Isa[2*], Vicinisvarri Inderan[3], Wan Zuraida Wan Kamis[4], Mustaffa Ali Azhar Taib[5]

[1,2,3,4]*Faculty of Chemical Engineering, Universiti Teknologi MARA, Cawangan Pulau Pinang, 13500 Permatang Pauh, Pulau Pinang, Malaysia*
[5]*Kolej Teknologi Termaju (ADTEC) JTM Kampus Taiping, PT15643, Kamunting Raya, Mukim Asam Kumbang, 34600 Kamunting, Perak, Malaysia*

ARTICLE INFO

Article history:
Received 14 January 2026
Revised 18 April 2026
Accepted 11 August 2026
Online first 20 September 2026
Published 20 September 2026

Keywords:
Electrodeposition
Tin/Indium composite electrode
Surface morphology
Elemental composition
X-ray diffraction

DOI:

10.24191/esteem.
v22iSeptember.10141

ABSTRACT

In this study, Indium-modified tin (Sn/In) electrodes were fabricated via electrodeposition using different $InCl_3$ precursor concentrations (0.01, 0.05 and 0.10) to study their effects on surface morphology, elemental composition and crystal structure. The prepared electrodes were analysed using scanning electron microscopy (SEM), energy-dispersive X-ray spectroscopy (EDX), X-ray fluorescence (XRF) and X-ray diffraction. SEM images showed that the 0.01 M $InCl_3$ electrode had patchy indium deposits with incomplete surface coverage, while the 0.05 M setup created a more uniform and continuous surface morphology. Increasing the concentration to 0.10 M led to particle clumping and higher surface roughness. Based on EDX data, the highest surface indium loading (15.86%) was achieved at 0.05 M, whereas XRF patterns XRF data showed a steady increase in bulk indium incorporation with higher precursor concentrations. The XRD patterns revealed that all Sn/In electrodes retained their tetragonal β-Sn crystal structure, and there was no other form of indium crystalline present in the sample. These results confirmed that the concentration of $InCl_3$ has played a key role in controlling the structural and compositional characteristics of electrodeposited Sn/In electrodes. Based on the results obtained, the electrode modified with 0.05 M $InCl_3$ offered the best balance between surface uniformity, indium loading and structural stability, making it a prospective candidate for subsequent electrochemical ethanol sensing applications.

[1*]Corresponding author. *E-mail address*: norain012@uitm.edu.my

1. INTRODUCTION

Tin is a material that is widely used in electrochemical applications. This is because tin has good electrical conductivity, chemical stability, low cost and a simple fabrication process [1-2]. From all these properties, tin is suitable for electrochemical sensors, electrocatalytic systems and energy storage devices [1]. However, unmodified tin has a relatively smooth surface that can limit the number of electrochemically active sites and reduce overall electrode performance [3].

Surface morphology, elemental composition and crystal structure determine electrode performance by directly shaping charge transfer and interfacial reactions [4]. Surface modification is widely used to improve the performance of tin electrodes while maintaining the advantages of the substrate. To understand how fabrication conditions shape modified metallic and oxide electrodes, accurate structural and compositional profiling must be deployed [5-6]. A common strategy is to incorporate a secondary metal to increase the number of active sites and improve electrochemical performance [7]. Indium is well suited for tin because both metals have compatible properties and can be co-electrodeposited under controlled conditions [8], [9]. Previous studies have shown that indium can improve surface characteristics without affecting the structural stability of the tin substrate[10-11].

Compared to other fabrication techniques, electrodeposition provides a straightforward and low-temperature process that can easily control coating thickness, composition and surface morphology [5], [12]. Several factors shape the quality of the deposited layer, which are the applied potential, deposition time, electrolyte composition, temperature and precursor concentration [12-13].It is important to have precursor concentration because it controls the supply of metal ions to the electrode surface, affecting nucleation, crystal growth and coating uniformity [12]. Precursor concentration requires a careful balance, as low concentrations limit ion availability and cause incomplete deposition, whereas excessive amounts tend to clump particles together and ruin coating uniformity [13-14].

Previous studies on indium electrodeposition have mainly focused on deposition mechanisms, electrochemical behaviour and process optimisation [8], [15]. In contrast, some studies have examined how indium precursor concentration influences the combined effects on the surface morphology, elemental composition and crystal structure of Sn/In electrodes [11]. Understanding this relationship is important to optimise electrode fabrication parameters and ultimately achieve a highly uniform and stable electrode surface. In this study, the fabrication of indium-modified tin (Sn/In) composite electrodes was carried out using a straightforward two-electrode electrodeposition method by varying the concentrations of $InCl_3$ precursor. The effect of indium doping concentrations on the surface morphology of the electrode, element composition and crystal structure was carefully studied using various types of analysis, including SEM, EDX, XRF and XRD. Based on this research, the electrode fabricated with 0.05 M $InCl_3$ exhibited the most uniform surface, which was considered the optimal deposition condition.

2. RESEARCH METHODOLOGY

2.1 Preparation of indium-modified tin (Sn/In) electrodes

In this study, indium-modified tin (Sn/In) electrodes were prepared using a commercial tin (Sn) foil as the substrate. The foil was cut into rectangular pieces with dimensions of 4.00 cm × 1.00 cm × 0.05 cm. Before electrodeposition, the Sn substrates were mechanically polished using 1000 – 1200 grit silicon

carbide (SiC) abrasive paper to remove surface contaminants and the native oxide layer. This pretreatment produced a clean and uniform surface for subsequent indium deposition. This surface preparation is commonly used in electrode fabrication to improve adhesion between the substrate and the deposited layer while providing better deposition quality [2], [16]. The polished substrates were cleaned in acetone using an ultrasonic bath for 10 min to remove any remaining contaminants. They were then cleaned in absolute ethanol for another 10 min and allowed to air-dry at room temperature before electrodeposition.

Besides, the cleaned Sn substrates were activated by immersion in 0.5 M sodium hydroxide (NaOH) solution for 30 – 60 s. This alkaline treatment modifies the surface and increases its suitability for the subsequent electrodeposition process. Similar surface preparation methods have been reported to improve surface quality and promote more uniform coatings during metal electrode fabrication [2], [16]. After the activation process, the substrates were thoroughly rinsed with deionised (DI) water that had been washed with ethanol and allowed to air-dry.

Next, electrodeposition was carried out using a two-electrode configuration with aqueous indium chloride ($InCl_3$) electrolyte solutions prepared in deionised (DI) water at concentrations of 0.01, 0.05 and 0.10 M. The pre-treated Sn foil was used as the cathode, while a platinum (Pt) plate served as the counter electrode (anode) (Fig. 1).

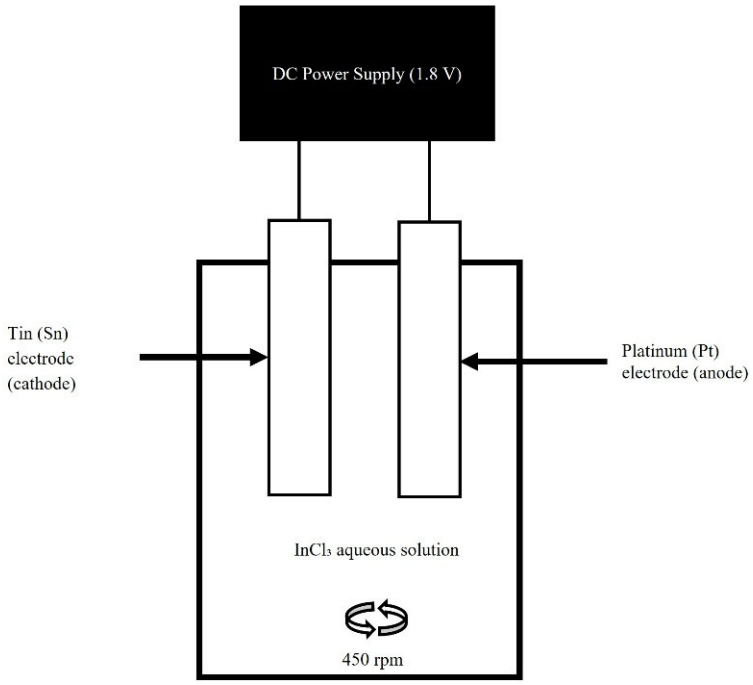

Fig. 1. Schematic illustration of the electrodeposition setup for Sn/In composite electrodes.

The deposition process was conducted in a glass electrochemical cell at a constant DC voltage of 1.8 V for 10 min. The electrolyte was continuously stirred at 450 rpm to maintain a uniform ion distribution.

This stirring condition helps to reduce concentration polarisation and promote more uniform growth of the indium coating on the Sn electrode surface.

Several electrodeposition parameters affect the quality of the deposited Sn/In layer, including electrolyte composition, applied voltage, deposition time and mass transport [12-13]. Among these, the $InCl_3$ precursor concentration is important because it determines the amount of indium ions available for deposition, which affects the nucleation process and subsequent coating growth. Therefore, proper control of the $InCl_3$ precursor concentration is crucial for achieving a homogeneous Sn/In electrode surface.

After electrodeposition, the Sn/In electrodes were removed from the electrolyte, then rinsed thoroughly with DI water and ethanol to eliminate residual salts and dried in an oven at 70 °C for about 40 – 45 min. The prepared electrodes were then characterised using scanning electron microscopy (SEM), energy-dispersive X-ray spectroscopy (EDX), X-ray fluorescence (XRF) and X-ray diffraction (XRD). These techniques were used to examine the effects of $InCl_3$ concentration on surface morphology, elemental composition and crystal structure (Fig. 2).

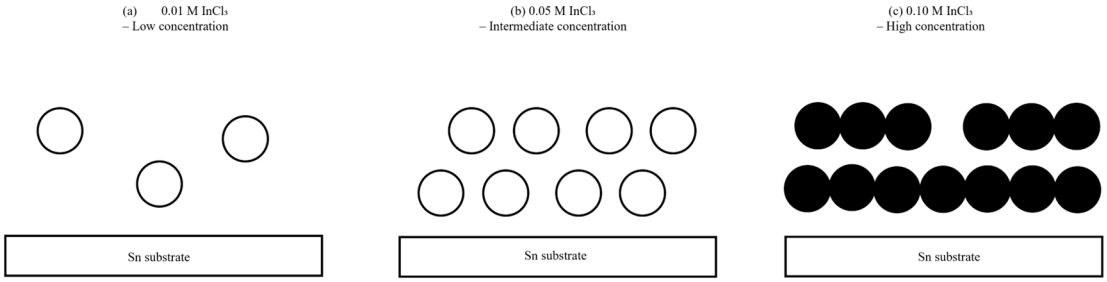

Fig. 2. Schematic of indium nucleation behaviour at different $InCl_3$ concentrations.

2.2 Structural and surface characterisation

The surface morphology and microstructure of the prepared Sn/In electrodes were characterised using field-emission scanning electron microscopy (FESEM, FEI Quanta FEG 650). Images were obtained at accelerating voltages of 5 – 10 kV to examine surface features, particle distribution, and the morphology of the electrodeposited indium layer. This technique provides detailed information on the deposited coating and is widely used to assess the effects of electrodeposition conditions on coating uniformity, particle distribution and deposit morphology [12], [17].

Surface elemental composition was analysed using energy-dispersive X-ray spectroscopy (EDX) integrated with the FESEM system. The relative weight percentages of tin (Sn) and indium (In) were determined from the selected surface regions according to the ASTM E1508-12a standard. EDX provides localised elemental information and is widely used to assess element incorporation and compositional changes in electrodeposited metal coatings [9], [11].

The crystal structure and phase composition of the Sn/In electrodes were characterised by X-ray diffraction (XRD) using a Rigaku Ultima IV diffractometer equipped with Cu Kα radiation ($\lambda = 1.5406$ Å). Diffraction patterns were compared with reference data from the International Centre for Diffraction Data (ICDD) database to identify crystalline phases and assess structural changes after indium deposition. XRD

is widely applied to investigate phase composition and crystallographic characteristics of tin- and indium-based electrode materials [2], [11].

Bulk elemental composition was further analysed using X-ray fluorescence (XRF) spectroscopy (Skyray Explorer 5000). The analysis was performed at an excitation voltage of 45.8 kV with an anode current of 40.16 mA under fixed operating conditions. In this study, XRF was selected to study the overall elemental composition of the electrodes instead of EDX, which provides only a localised surface analysis [18].

3. RESULTS AND DISCUSSION

3.1 Surface morphology analysis of electrodeposited Sn/In electrodes

The scanning electron microscopy (SEM) micrographs of the electrodeposited Sn/In electrodes are presented in Fig. 3. The effect of the $InCl_3$ precursor concentration on the surface morphology of the electrodes was examined. The bare Sn substrate, before electrodeposition (Fig. 3(a)), showed a relatively smooth surface with distinct parallel polishing marks produced during surface preparation. This surface characteristic provides a useful reference for analysing the surface morphology modification upon the introduction of indium deposition.

During electrodeposition at 0.01 M $InCl_3$ (Fig. 3(b)), indium deposits appeared as scattered islands across the Sn surface, leaving some areas of the substrate exposed. This discontinuous layer suggests that the low precursor concentration provided insufficient In^{3+} ions for widespread nucleation and growth, resulting in partial surface coverage. Similar behaviour has been reported for electrodeposited metal coatings, where limited metal-ion availability can reduce nucleation density and produce non-uniform deposits [9], [15], [19].

Increasing the $InCl_3$ concentration to 0.05 M (Fig. 3(c)) produced a different surface morphology. The deposited layer was more compact and uniformly distributed, with better surface coverage and less particle agglomeration. This suggests that the intermediate precursor concentration provided sufficient In^{3+} ions for more uniform nucleation while allowing controlled crystal growth. These conditions support the formation of a continuous coating and are consistent with previous studies showing that suitable electrolyte composition can improve deposit uniformity by balancing ion transport and surface growth during electrodeposition [2], [5], [12].

Further increasing the precursor concentration to 0.10 M (Fig. 3(d)) resulted in larger and more irregular particle clusters on the electrode surface. Instead of improving surface coverage, the higher supply of In^{3+} ions appeared to promote further growth at existing nucleation sites, leading to particle agglomeration and a rougher surface. This change from a relatively uniform coating to clustered deposits reflects the change in the balance between nucleation and crystal growth that can occur at higher precursor concentrations during electrodeposition [9], [12], [17].

Overall, the SEM observations demonstrate that the $InCl_3$ precursor concentration strongly influences the morphology of electrodeposited Sn/In electrodes. The 0.01 M electrolyte produced an incomplete and discontinuous indium coverage, whereas the 0.10 M electrolyte demonstrated particle aggregation that reduced the coating uniformity. In contrast, the electrode prepared with 0.05 M $InCl_3$ showed the most homogeneous surface morphology. Thus, it suggests that this concentration provides the most favourable

conditions for controlled indium deposition. The elemental and structural analyses presented in the following sections further support these morphological characteristics.

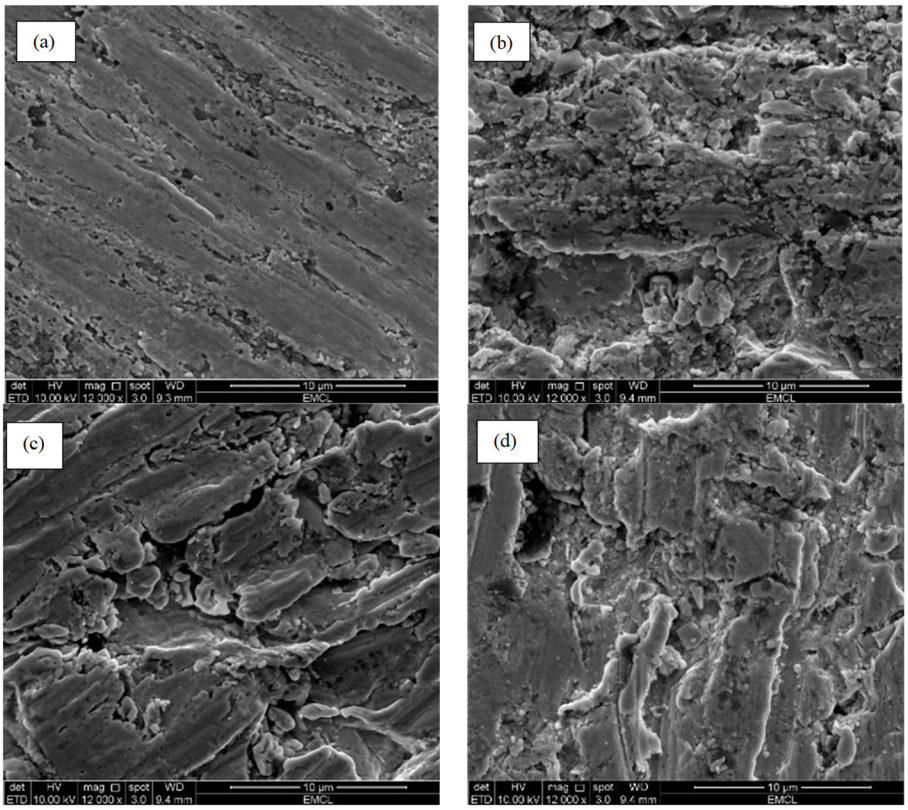

Fig. 3. SEM images of (a) bare Sn, (b) Sn/In (0.01 M), (c) Sn/In (0.05 M), and (d) Sn/In (0.10 M) electrodes.

3.2 Elemental composition analysis of Sn/In electrodes

The elemental composition of the fabricated electrodes was evaluated using both energy-dispersive X-ray spectroscopy (EDX) and X-ray fluorescence (XRF). The EDX results summarised in Table 1 provide information on the elemental composition of the electrode surface, whereas the XRF data in Table 2 represent the bulk composition of the samples. Because these techniques investigate a different region of the material, their combined use offers a more comprehensive understanding of indium incorporation following electrodeposition [11], [18].

Table 1. Surface elemental composition (wt.% and at. %) of bare Sn and Sn/In electrodes determined by EDX.

Sample	O (wt.%)	In (wt.%)	Sn (wt.%)	O (at. %)	In (at. %)	Sn (at. %)
Bare Sn	2.11	0.00	97.89	13.76	0.00	86.24
Sn/In (0.01 M)	4.73	9.85	85.41	26.87	7.79	65.34
Sn/In (0.05 M)	5.92	15.86	78.23	31.69	11.84	56.48
Sn/In (0.10 M)	8.53	11.98	79.50	40.78	7.98	51.24

Table 2. Bulk elemental composition of Sn/In electrodes determined by XRF (mean ± SD).

Element	0.01 M Sn/In	0.05 M Sn/In	0.10 M Sn/In
Fe (%)	0.29 ± 0.02	0.21 ± 0.10	0.21 ± 0.11
Ni (%)	0.05 ± 0.01	0.04 ± 0.03	0.04 ± 0.03
Cu (%)	0.17 ± 0.01	0.18 ± 0.04	0.18 ± 0.02
Zn (%)	0.03 ± 0.01	0.01 ± 0.01	0.23 ± 0.40
As (%)	0.00 ± 0.00	0.00 ± 0.00	0.00 ± 0.00
Se (%)	0.00 ± 0.00	0.00 ± 0.00	0.00 ± 0.00
Ag (%)	0.00 ± 0.00	0.00 ± 0.00	0.00 ± 0.00
Cd (%)	0.14 ± 0.04	0.18 ± 0.10	0.21 ± 0.07
In (%)	0.26 ± 0.05	0.33 ± 0.15	0.36 ± 0.10
Sn (%)	93.62 ± 0.77	93.02 ± 1.90	92.49 ± 1.14
Sb (%)	0.33 ± 0.16	0.53 ± 0.49	0.59 ± 0.28
Hg (%)	0.01 ± 0.00	0.01 ± 0.00	0.01 ± 0.00
Pb (%)	5.00 ± 0.49	5.37 ± 1.19	5.55 ± 0.77
Bi (%)	0.01 ± 0.01	0.01 ± 0.01	0.01 ± 0.01

Data are presented as mean ± SD. Measurements were performed in quintuplicate (n = 5) for all samples except the 0.10 M Sn/In electrode (n = 4) due to one invalid measurement.

The EDX spectrum of the bare Sn electrode showed a dominant tin signal with no detectable indium, confirming the absence of surface modification important to electrodeposition (Fig. 4). Analysis detected a small amount of oxygen (2.11 wt.%), which comes from the natural oxide layer formed on the tin surface after air exposure. Metallic tin commonly shows this surface oxidation, which does not mean a significant bulk oxide phase has formed [20].

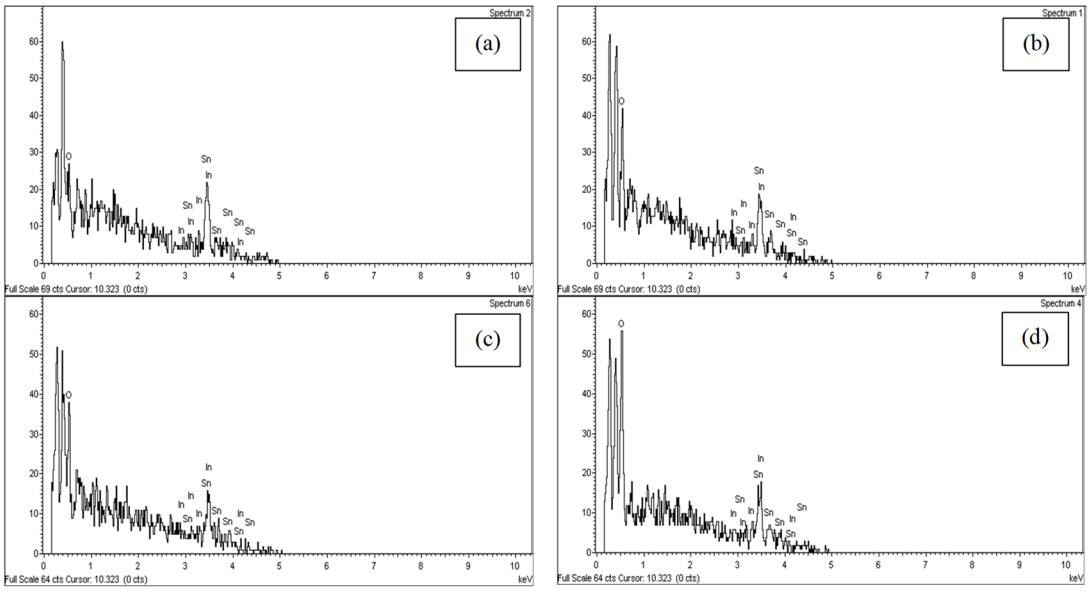

Fig. 4. EDX spectra and elemental composition of (a) bare Sn, (b) 0.01 M Sn/In, (c) 0.05 M Sn/In, and (d) 0.10 M Sn/In electrodes.

Following electrodeposition, indium was found in all Sn/In electrodes, showing that the process successfully added indium to the surface. When the $InCl_3$ precursor concentration rose from 0.01 M to 0.05 M, the surface indium content increased from 9.85 wt.% to 15.86 wt.%. This trend matches the SEM data, where the 0.05 M electrode showed the most uniform surface coverage. The higher indium loading suggests that sufficient In^{3+} ions drove continuous nucleation and even deposition. Past studies show similar links between precursor concentration, ion availability, and metal deposition [9], [12].

Interestingly, a precursor concentration of 0.10 M did not raise the surface indium content further. Instead, the measured indium concentration fell to 11.98 wt.% despite the higher $InCl_3$ concentration in the electrolyte. This behavior shows that too many ions alter the deposition process, favoring local particle growth over uniform coverage. Consequently, indium aggregates in specific regions instead of spreading evenly. This matches the SEM images, which showed clear particle clustering at the highest concentration, and agrees with earlier reports on nucleation changes in highly concentrated baths [9], [17].

The oxygen content also climbed progressively after deposition, rising from 2.11 wt.% (bare Sn) to 8.53 wt.% (0.10 M Sn/In). This rise likely stems from the larger surface area of the indium structures, which offers more sites for air adsorption and oxidation. Since XRD found no oxide phases, the oxygen is likely due to surface passivation rather than bulk oxide formation [20].

XRF data confirmed that tin remained the main component, making up over 92 wt.% of the total mix. Unlike the EDX data, the bulk indium content rose slowly from 0.26 ± 0.05 wt.% (0.01 M sample) to 0.36 ± 0.10 wt.% (0.10 M sample). Trace amounts of Pb, Sb, Fe, Cu, and Ni were also found, coming from the original Sn foil. These steady concentrations show that the modification affected only the surface and did not change the bulk metal substrate.

The different indium levels highlight the different sampling depths of the two tools. EDX measures the surface, while XRF averages the bulk material [11], [18]. Thus, the higher indium levels in EDX confirm that indium clustered at the surface layer rather than distributing evenly through the Sn substrate. This shows that the process modified the surface while preserving the bulk properties of the underlying tin, supporting later sensing applications.

3.3 Crystal structure and phase evolution of Sn/In electrodes

X-ray diffraction (XRD) was used to study the crystal structure of the bare Sn and electrodeposited Sn/In electrodes, and Fig. 6 shows the patterns. The bare Sn substrate exhibited characteristic diffraction peaks at approximately 30.9°, 32.25°, 44.1°, 45.13°, 55.56°, 55.74°, 62.7°, 64.8°, 72.6°, 73.35° and 79.73° corresponding to the (200), (101), (220), (211), (031), (112), (400), (240), (141) and (321) crystallographic planes of tetragonal β-Sn (space group $I4_1/amd$, COD 1534488). These results prove that the commercial Sn foil kept its expected crystalline form before surface modification, which matches past studies on tin-based metals [21].

Following electrodeposition, all Sn/In electrodes showed diffraction patterns that closely mirrored the bare Sn substrate. No major peak shifts, broadening, or extra peaks were seen after modification. This stability proves that the process did not alter the bulk crystal structure of the Sn substrate. This finding shows that indium depositions stayed mainly at the surface while preserving the structural setup of the β-Sn matrix. Past work shows similar trends for Sn-based electrodes with low indium levels, where surface changes occur without hurting the bulk crystal structure [19].

Analysis also showed a total absence of diffraction peaks for crystalline indium, indium oxide, or Sn–In compounds across all modified electrodes. This trend matches the EDX and XRF data, which showed low amounts of surface indium compared to the large Sn substrate. The deposited indium is likely a thin surface layer or exists in amounts below the XRD detection limit, which prevents distinct crystalline peaks. [19].

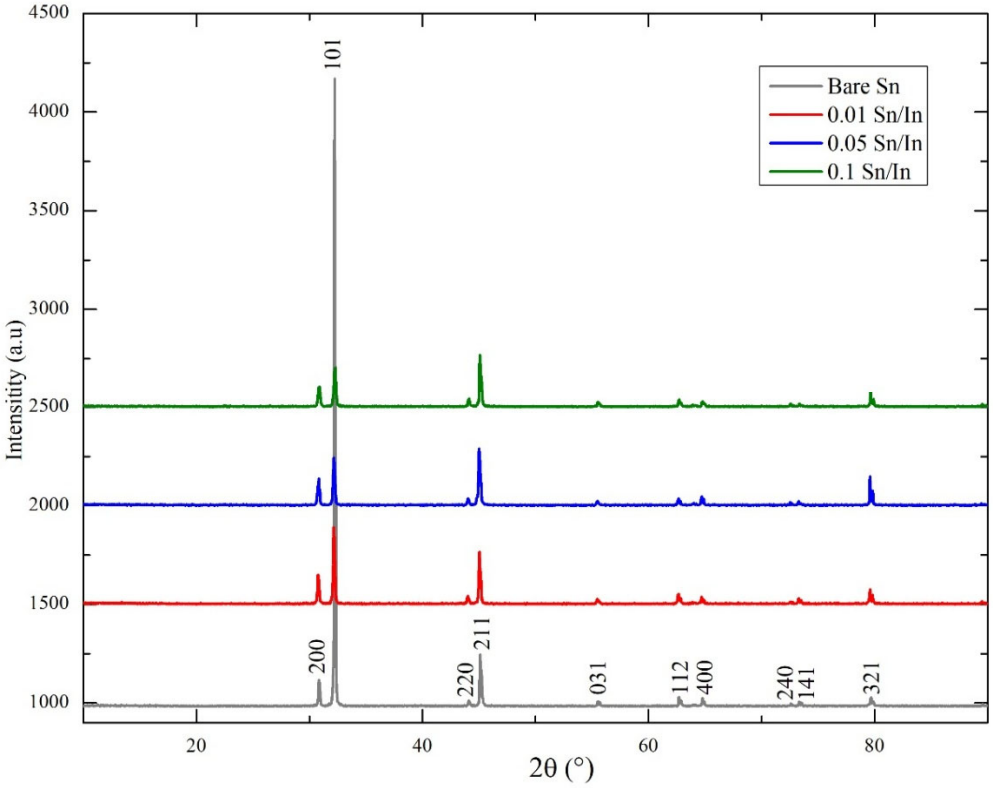

Fig. 6. X-ray diffraction patterns of bare Sn and Sn/In composite electrodes prepared at different indium precursor concentrations.

Peak overlap between both metals explains the missing indium peaks. The typical In (101) peak appears near 32.9°, which sits very close to the strong β-Sn (101) peak at 32.25°. Thus, the stronger Sn substrate signal hides the indium signal, especially when the indium layer is thin or scattered. This point supports the view that indium acts as a surface modifier rather than a separate crystalline phase [19].

Although the overall shapes stayed similar, the modified electrodes showed small changes in peak intensity. Specifically, the 0.10 M Sn/In electrode showed a slight drop in (101) and (200) intensity compared to the 0.05 M sample. The higher surface roughness and particle clustering seen in SEM likely caused this drop, as rough surfaces lower diffraction intensity by adding structural disorder [19]. Conversely, the modified electrodes gave stronger (101) peaks than the bare Sn substrate. This change

suggests that indium influenced the direction of crystal growth during electrodeposition, even though the overall β-Sn crystal structure stayed the same.

Overall, the XRD data demonstrates that changing the $InCl_3$ precursor concentration alters the surface features without changing the crystal structure of the Sn substrate. The retention of the tetragonal β-Sn phase fits the trends seen in the SEM, EDX, and XRF results. Collectively, these findings indicate that indium was successfully deposited as a stable surface layer while maintaining the structural integrity of the underlying Sn electrode, which is an important characteristic for subsequent electrochemical ethanol sensing applications.

3.4 Correlation between indium concentration, surface morphology, and structural characteristics of Sn/In electrodes

The combined SEM, EDX, XRF and XRD data clearly prove that the $InCl_3$ precursor concentration determines the structural and compositional features of electrodeposited Sn/In electrodes. Although the bulk crystal structure of the Sn substrate remained unchanged during the process, variations in precursor concentration strongly altered indium deposition behaviour, surface morphology, and elemental distribution. These trends highlight the need to precisely control electrolyte composition to achieve a uniform, stable electrode [2], [12], [19].

At the lowest concentration of 0.01 M, the limited supply of In^{3+} ions restricted nucleation, causing a discontinuous indium layer across the Sn surface. This outcome was clearly visible in the SEM images, which showed isolated deposits and incomplete surface coverage, while the low surface indium content measured by EDX further supports this finding. The data suggest that low ion availability blocked the growth of a continuous coating, subsequently leading to a less uniform surface [8], [14]. Past work shows similar trends for dilute baths, where low metal-ion concentrations suppress nucleation density and lower coating uniformity [12-13].

Raising the precursor concentration to 0.05 M produced a major improvement in the deposited layer. A compact and uniform surface was observed via SEM, while EDX data recorded the highest surface indium content among all tested electrodes. Concurrently, the XRD patterns stayed essentially unchanged, confirming that indium deposition was strictly confined to the surface without altering the tetragonal β-Sn crystal structure [11], [19], [21]. The match between these characterisation tools shows that 0.05 M balances ion availability, nucleation, and crystal growth, thereby allowing indium to spread evenly. Similar trends have been reported before, where intermediate precursor concentrations actively promoted uniform deposition and better coating quality [12], [15], [17].

Further increasing the $InCl_3$ concentration to 0.10 M altered the deposition behaviour. Instead of improving surface coverage, the excess In^{3+} ions drove preferential growth at existing nucleation sites, yielding particle clusters and a rougher surface morphology [7], [12], [17]. This observation fits the lower surface indium content found by EDX compared to the 0.05 M electrode, despite the slow bulk indium increase tracked by XRF. The difference between the surface and bulk datasets suggests that extra indium deposited unevenly rather than spreading uniformly. Such behaviour is commonly linked with a shift from nucleation-controlled to growth-dominated deposition under high precursor concentrations [12], [17].

Despite different surface shapes and element distributions, the typical diffraction peaks of tetragonal β-Sn were kept by all modified electrodes, showing no traces of crystalline indium, indium oxide, or Sn–

In intermetallic phases [11], [19], [21]. This confirms that the process changed the outer surface primarily while keeping the structural integrity of the Sn substrate. The matching data from EDX and XRF further validate this conclusion, which shows that indium is concentrated at the surface layer rather than dispersing through the bulk material [18], [19].

Overall, the results prove that controlling the $InCl_3$ precursor concentration is essential for shaping the surface features of electrodeposited Sn/In electrodes. Among the concentrations tested, the electrode made with 0.05 M $InCl_3$ showed the best mix of uniform surface morphology, highest surface indium integration, and excellent structural stability. These attributes make the 0.05 M Sn/In electrode the most promising choice for later electrochemical ethanol sensing tests, where a uniform and stable electrode surface is expected to boost sensing performance.

4. CONCLUSION

This study clearly demonstrated that the $InCl_3$ precursor concentration strongly influences the structural and compositional characteristics of electrodeposited Sn/In electrodes. At 0.01 M, incomplete surface coverage was caused by limited indium availability, while increasing the concentration to 0.10 M actively promoted particle agglomeration and reduced coating uniformity. In contrast, the electrode prepared with 0.05 M $InCl_3$ exhibited the most favourable characteristics, including a uniform surface morphology, the highest surface indium incorporation, and full preservation of the tetragonal β-Sn crystal structure without the formation of secondary crystalline phases. The combined SEM, EDX, XRF and XRD analyses confirm that precursor concentration governs indium deposition behaviour while maintaining the structural integrity of the Sn substrate. These findings demonstrate that optimising the $InCl_3$ concentration is essential for producing structurally stable and compositionally uniform Sn/In electrodes. The optimised 0.05 M Sn/In electrode, therefore, provides a reliable foundation for subsequent electrochemical ethanol sensing studies.

5. ACKNOWLEDGEMENTS/FUNDING

This research was funded by the Ministry of Higher Education Malaysia under the Fundamental Research Grant Scheme (FRGS) [Grant No. FRGS/1/2023/TK09/UITM/02/26]. The authors sincerely thank Materials Technology, Department of Manufacturing & Advanced Materials, ADTEC Taiping, Malaysia, for their support with XRD and XRF analyses.

6. CONFLICT OF INTEREST STATEMENT

The authors declare that this research was conducted in the absence of any commercial or financial relationships that could be construed as a potential conflict of interest. The funders had no role in the design of the study, data collection and analysis, interpretation of results, or decision to publish the findings.

7. AUTHORS' CONTRIBUTIONS

Nur Basiroh Mohd Rahim: Conceptualisation, methodology, investigation, data curation, formal analysis, and writing – original draft. Norain Isa: Conceptualisation, supervision, validation, and writing – review and editing. Vicinisvarri Inderan: Supervision, validation, and writing – review and editing. Wan Zuraida

Wan Kamis: review and editing. Mustaffa Ali Azhar Taib: review and editing. All authors have read and approved the final manuscript.

8. DECLARATION OF GENERATIVE AI IN THE WRITING PROCESS

During the preparation of this work, the authors used ChatGPT (OpenAI) to refine grammatical structures, improve language clarity, and enhance overall readability of the technical discussions. After using this tool/service, the authors reviewed and edited the content as needed and took full responsibility for the content of the publication.

9. DATA AVAILABILITY/SUPPLEMENTARY MATERIALS

The datasets used and/or analysed during the current study are available from the corresponding author on reasonable request.

10. ETHICS STATEMENT

The authors declare that this research did not involve human or animal subjects. All experimental procedures were performed following the institutional Safety, Health, and Environmental (HSE) protocols of Universiti Teknologi MARA (UiTM).

11. REFERENCES

[1] H. J. Nsaif and N. S. Majeed, "Modified Graphite with Tin Oxide as a Promising Electrode for Reduction of Organic Pollutants from Wastewater by Sonoelectrochemical Oxidation," *Ecol. Eng. Environ. Technol.*, vol. 25, no. 1, pp. 307–320, 2024. Available: https://doi.org/10.12912/27197050/175437

[2] X. Cao *et al.*, "Electrochemical behavior and electrodeposition of sn coating from choline chloride–urea deep eutectic solvents," *Coatings*, vol. 10, no. 12, pp. 1–10, 2020. Available: https://doi.org/10.3390/coatings10121154

[3] C. Albenga *et al.*, "Assessing the role of morphological changes as the origin of improved cycling stability of Sn-based anodes for sodium-ion batteries," *J. Mater. Chem. A*, vol. 13, no. 37, pp. 30967–30984, 2025. . Available: https://doi.org/10.1039/d5ta03000e

[4] A. V. Stanchik *et al.*, "Morphology and Crystal Structure of Cu2NiSn(S,Se)4 Thin Films Obtained by an Electrodeposition-Annealing Process," *Coatings*, vol. 12, no. 8, 2022. Available: https://doi.org/10.3390/coatings12081198

[5] E. Arulkumar, S. Thanikaikarasan, and N. Tesfie, "Influence of Deposition Parameters for Cu2O and CuO Thin Films by Electrodeposition Technique: A Short Review," 2023, *Hindawi Limited*. Available: https://doi.org/10.1155/2023/8987633

[6] N. A. Abdul Wahab *et al.*, "Influence of iron doping on the morphological and compositional properties of zirconia foil as photocatalyst," *ESTEEM Acad. J.*, vol. 21, no. March, pp. 59–73, 2025. Available: https://doi.org/ 10.24191/esteem.v21imarch.586.g3074

[7] Y. Su, N. Chen, H. L. Ren, L. L. Guo, Z. Li, and X. M. Wang, "Preparation and Properties of Indium Ion

Modified Graphite Felt Composite Electrode," *Front. Chem.*, vol. 10, no. April, pp. 1–7, 2022. Available: https://doi.org/10.3389/fchem.2022.899287

[8] Z. Hou, X. Wang, J. Li, Z. Li, Y. Wang, and H. Xing, "Electrochemical Mechanism of the Preparation of High-Purity Indium by Electrodeposition," *Front. Chem.*, vol. 10, no. May, pp. 1–8, 2022. Available: https://doi.org/ 10.3389/fchem.2022.871420

[9] Z. Hou, J. Li, X. Wang, Y. Wang, H. Xing, and Z. Li, "Effect of Tin Ion on Electrodeposition Behavior of Indium," *Electrochemistry*, vol. 90, no. 8, pp. 1–6, 2022. Available: https://doi.org/10.5796/electrochemistry.22-00051

[10] S. M. Yang, H. K. Yen, and K. C. Lu, "Synthesis and Characterization of Indium Tin Oxide Nanowires with Surface Modification of Silver Nanoparticles by Electrochemical Method," *Nanomaterials*, vol. 12, no. 6, pp. 0–11, 2022. Available: https://doi.org/10.3390/nano12060897

[11] T. Dobrovolska *et al.*, "Development and Characterization of Electrodeposited Tin-Indium Alloy Microbumps for Low Temperature Assembly," *Proc. - Electron. Components Technol. Conf.*, pp. 1924–1928, 2025. Available: https://doi.org/10.1109/ECTC51687.2025.00328

[12] M. Hu, Y. Wang, Z. Chen, S. Ning, and Y. Wei, "Study of Indium electrodeposition and nucleation mechanism in acidic solution using EQCM," *Electrochim. Acta*, vol. 443, no. October 2022, p. 141963, 2023. Available: https://doi.org/10.1016/j.electacta.2023.141963

[13] C. Lupi, E. Ciro, and A. Dell'Era, "Study of Operational Parameters on Indium Electrowinning Using a Ti Cathode," *Materials (Basel).*, vol. 18, no. 9, pp. 1–19, 2025. Available: https://doi.org/10.3390/ma18092089

[14] S. Li, H. Wang, S. Wang, F. Xie, and X. Sun, "Ultrasound-assisted electrodeposition of indium from HCl stripped indium-loaded organic phase solutions by EQCM: Electrochemical behavior and nucleation mechanisms," *Ultrason. Sonochem.*, vol. 119, no. March, p. 107410, 2025. Available: https://doi.org/10.1016/j.ultsonch.2025.107410

[15] E. Ciro, A. Dell'Era, and C. Lupi, "Indium electrowinning on Al cathode: Tuning of operating parameters and obtained deposits characterization," *J. Environ. Chem. Eng.*, vol. 14, no. 2, p. 121471, 2026. Available: https://doi.org/ 10.1016/j.jece.2026.121471

[16] O. Ait Layachi *et al.*, "Electrodeposition of Cu2NiSnS4 absorber layer on FTO substrate for solar cell applications," *RSC Adv.*, vol. 14, no. 40, pp. 29439–29454, 2024. Available: https://doi.org/10.1039/d4ra04249b

[17] X. Liu *et al.*, "Study on the Optimization of the Morphology and Nucleation Mechanism of Electroplated Sn-Pb Coatings by the Synergistic Effect of Composite Additives," *Metals (Basel).*, vol. 15, no. 9, 2025. Available: https://doi.org/10.3390/met15090936

[18] F. Ren *et al.*, "X-ray fluorescence spectroscopy for rapid identification of cathode chemistry in lithium-ion battery recycling," *Commun. Eng.*, vol. 5, no. 1, pp. 1–12, 2026. Available: https://doi.org/10.1038/s44172-026-00618-3

[19] N. G. Sousa *et al.*, "Modelling approach applied to SnIn coatings from choline chloride/ethylene glycol deep eutectic solvent," *J. Mol. Liq.*, vol. 390, no. PA, p. 122973, 2023. Available: https://doi.org/10.1016/j.molliq.2023.122973

[20] J. E. Martinez Medina, A. M. Philippe, J. Guillot, C. Vergne, Y. Fleming, and E. Barborini, "Intermediate tin oxide in stable core-shell structures by room temperature oxidation of cluster-assembled nanostructured Sn films," *Appl. Surf. Sci.*, vol. 658, no. January, p. 159846, 2024. Available: https://doi.org/10.1016/j.apsusc.2024.159846

[21] T. Malik, P. Cifligu, C. Park, and E. Evlyukhin, "X-ray induced synthesis of beta tin (β-Sn)," *J. Phys. Chem. Solids*, vol. 196, no. August 2024, p. 112351, 2025. Available: https://doi.org/10.1016/j.jpcs.2024.112351